Stable, High-Efficiency Voltage-Dependent Color-Tunable Organic Light-Emitting Diodes with a Single Tetradentate Platinum(II) Emitter Having Long Operational Lifetime

Mao Mao, Tsz-Lung Lam, Wai-Pong To, Xiang-Zhou Lao, Weiqiang Liu, Shi-Jie Xu, Gang Cheng, and Chi-Ming Che**

Dr. M. Mao, Dr. T. L Lam, Dr. W.-P. To, Dr. G. Cheng, W. Liu, Prof. C.-M. Che
State Key Laboratory of Synthetic Chemistry, HKU-CAS Joint Laboratory on New Materials, and Department of Chemistry, The University of Hong Kong, Pokfulam Road, Hong Kong SAR, P. R. China
E-mail: ggcheng@hku.hk, cmche@hku.hk

X.-Z. Lao, Prof. S.-J. Xu
Department of Physics, The University of Hong Kong, Pokfulam Road, Hong Kong SAR, P. R. China
Dr. X.-Z. Lao, Dr. G. Cheng, Prof. C.-M. Che
HKU Shenzhen Institute of Research and Innovation, Shenzhen 518053, P. R. China

Keywords: tetradentate Pt(II) complexes, organic light-emitting diodes, color-tunable, single emitter, high efficiency

Abstract: Voltage-dependent, color-tunable organic light-emitting diodes (OLEDs) are appealing tools that can be used for the visualization of electronic output signal of sensors. Nonetheless, the literature reported color-tunable OLEDs that have a simple single-cell device structure suffer from relatively low efficiency, pronounced efficiency roll-off, color-aging, and short operation lifetime, all of which limit practical applications. Here we describe a novel co-host-in-double-emissive-layer (CHIDEL) device, designed to enhance the performance of color-tunable OLEDs with the use of a single tetradentate Pt[O^N^C^N] emitter. When **Pt-X-2** was used as a single emitter in an optimized CHIDEL device, a white OLED with CIE tunable coordinates from (0.47, 0.44) at 3 V to (0.36, 0.48) at 11 V, a high color rendering index of 82, and high EQEs of up to 20.75% could be achieved. By using **Pt-X-4** as a single emitter, the voltage-dependent color-tunable CHIDEL device, with CIE coordinates shifted from (0.56, 0.43) at 3 V to (0.42, 0.55) at 11 V, demonstrated a high luminance of beyond 90000 cd m^{-2} and a high EQE of 23.23% at a luminance of 1300 cd m^{-2}. A long lifetime (LT_{90}) of almost 20000 h has been demonstrated for the color-tunable OLED with **Pt-X-4** emitting dopant.

After their commercial success in display panels, organic light-emitting diodes (OLEDs) are expected to play a critical role in next-generation solid-state illumination and smart lighting, owing to their unique properties, such as flexibility, ultra-thin thickness and light weight.[1-8] In addition to fixed chromaticity in ordinary illumination devices, there is a great demand for tunable chromaticity in certain applications, such as smart lighting, decoration and botanical grow lamps.[9-13] Specifically, the voltage-dependent, color-tunable OLED is an appealing tool for the visualization of the electronic output signal of sensors, such as real-time wearable electrocardiogram monitors and electronic skin sensors.[13,14] As shown in **Scheme 1**, several strategies for the construction of color-tunable OLEDs have been proposed in the literature.[9,10,12,13,15-23] Among these strategies, the most straightforward is the combination of multiple, independently controlled sub-OLED arrays in parallel or tandem way (Scheme 1a and 1b).[9,15-17] Reineke and co-workers designed a tandem color-tunable device structure with two independently controlled orange and blue sub-OLEDs that share a common electrode. This device can achieve a wide color-span range, from blue via white to orange, and has a high power efficacy (PE) of 36.8 lm W^{-1} by using alternating current as the power source.[17] Nonetheless, this kind of device has a sophisticated device structure, thereby leading to a potentially high fabrication cost and low long-term stability. A single-cell device structure with multiple emitters, that can be selectively activated at different driving voltages, is a simpler choice for color-tunable OLEDs.[10,12,13,18-23] Several mechanisms have been proposed in the literature to explain the color-shift phenomenon of this type of OLED, such as the move of the exciton recombination zone from one emitting layer (EML) to another, in the devices with multiple EMLs (Scheme 1c),[20] as well as a competition between charge-trapping emission and energy-transfer emission,[21] or the change of energy transfer rate between different emitters[23] in the devices with a single EML (Scheme 1d). Compared to the color-tunable OLEDs combined with multiple sub-OLEDs, the single-cell varieties usually possess relatively low efficiency and/or pronounced efficiency roll-off. For instance, although a high external quantum efficiency

(EQE) of up to 22.02% was achieved in a color-tunable OLED, by co-doping a yellow-emitting Au(III) complex and a blue-emitting Ir(III) complex in a shared host, the EQE value plummeted at high luminance due to the saturation of the emissive excited state of the Au(III) emitter.[23] In addition, the color-aging limitation potentially arises due to differential operating lifetimes of the multiple emitters used in the reported color-tunable OLEDs.[4,24] In principle, such a color-aging issue can be avoided by simplifying the device structure that requires only a single emitter (Scheme 1e). As the single emitter is the crucial component of this kind of device, a qualified one should fulfill two criteria; i) have the ability to emit both high-energy and low-energy light at the same time, in order to guarantee a wide color-span range; ii) exhibit high efficiency and short emission lifetime for both high-energy and low-energy emission to achieve high electroluminescent (EL) efficiency at a practical luminance of 1000 cd m^{-2}. Among the literature-reported high-efficiency emitters for OLEDs,[25-32] platinum(II) complexes can fulfill both criteria, due to their planar molecular structure: i) Pt(II) complexes have a strong propensity toward aggregation via π–π stacking and/or metal-metal interactions that give rise to new triplet metal-metal-to-ligand charge transfer (^{3}MMLCT) emission in the low-energy spectral region,[26,27] and ii) phosphorescence from Pt(II) emitters in aggregated forms generally features markedly enhanced radiative decay rate constants and much shorter emission lifetimes, compared to monomer emission, owing to the increased metal character in the emissive ^{3}MMLCT excited state.[30–32] Furthermore, with tetradentate ligands having C donor atom(s), structurally robust and high luminescent-efficiency tetradentate platinum(II) emitters could be developed.[25,27,28,32,33]

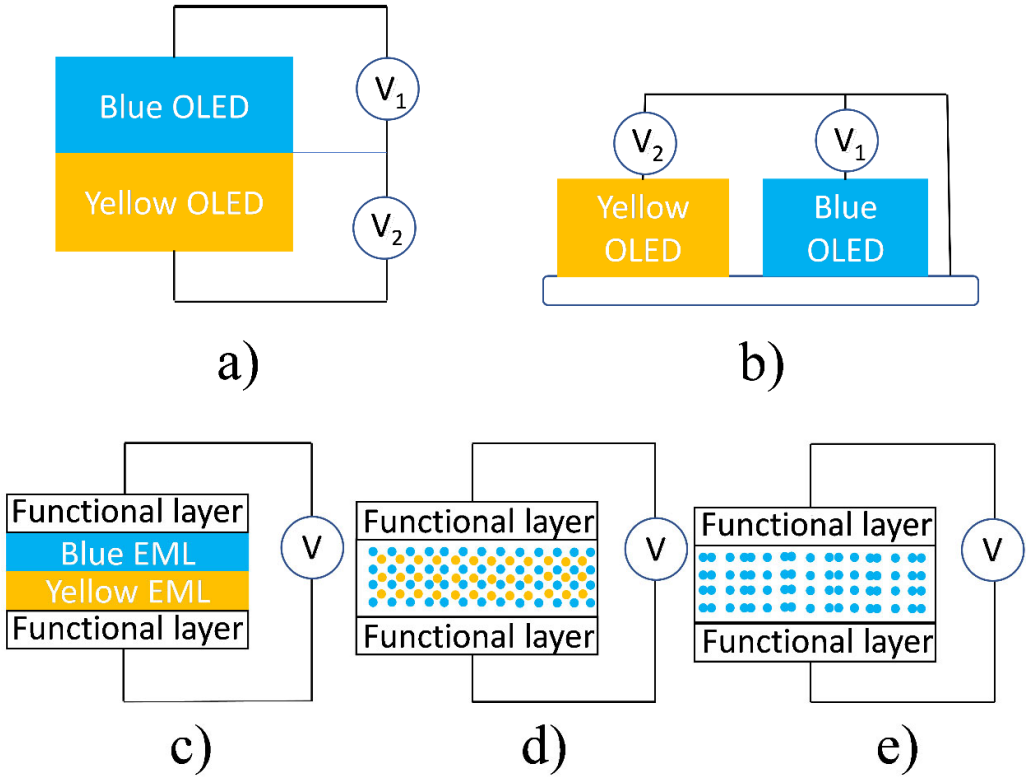

Scheme 1. Schematic diagrams of different strategies for color-tunable OLEDs. a) an independently controlled tandem sub-OLED array; b) an individually controlled parallel sub-OLED array; c) a single OLED cell with multiple emissive layers; d) a single OLED cell with multiple emitters in a single emissive layer; and e) a single OLED cell with a single emitter in a single emissive layer.

Recently, we have designed and synthesized a series of efficient phosphorescent Pt(II) emitters supported by tetradentate [O^N^C^N] ligands. High EQEs of up to 26.8% were achieved in OLEDs based on the emission of such Pt(II) complexes.[25,27,30] Among them, **Pt-X-2**, **Pt-X-3**, and **Pt-X-4** (**Scheme 2**) all have the potential for use as single emitting dopant in the fabrication of voltage-dependent, color-tunable OLEDs, owing to the outstanding EL performance of the Pt[O^N^C^N] complexes at both monomer and aggregation states.[30] In the present study, we describe high-performance, color-tunable OLEDs with low-efficiency roll-off and wide color-span range, with a novel device structure. When **Pt-X-4** was used as the single emitter, the emission color can be tuned from orange (3 V) to yellowish-green (11 V) with high EQEs of up to 23.23% and luminance beyond 90000 cd m^{-2}. At high luminance of

5000 and 10000 cd m^{-2}, efficiency roll-offs of the **Pt-X-4** devices were low, at 9.38% and 19.97%, respectively. For the white OLEDs fabricated with **Pt-X-2,** the Commission International de l'Eclairage (CIE) coordinates shifted from (0.47, 0.44) to (0.36, 0.48). In addition, a high color rendering index (CRI) of 82, maximum EQE of 20.75% and maximum PE of 50.18 lm W^{-1} were achieved with this device. At the practical luminance of 1000 cd m^{-2} for illumination devices, the EQE value slightly decreased to 19.96%, corresponding to a roll-off of 3.8%. We attribute this improved efficiency roll-off of both devices to the high efficiency and short emission lifetime of the Pt[O^N^C^N] in the aggregated state.[30] Theory simulation with the trapping-and-energy-transfer model indicates that such a color-tunable phenomenon in the OLEDs with a single Pt-emitter may be the result of competition between charge-trapping and energy-transfer emission mechanisms.

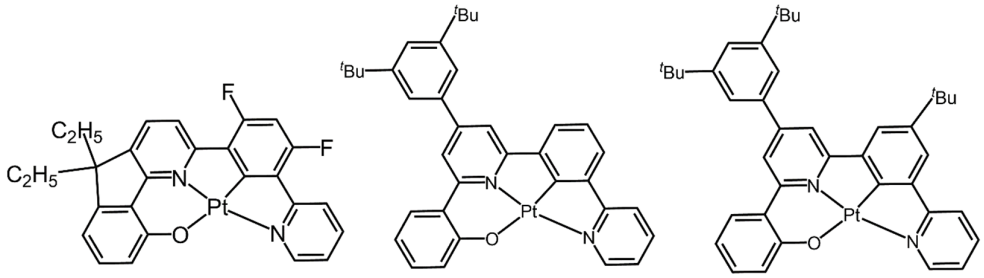

Scheme 2. Chemical structures of **Pt-X-2, Pt-X-3** and **Pt-X-4**.

Considering its relatively simple molecular structure and well-studied concentration-dependent emission, **Pt-X-3** was exploited to investigate the influence of device structure on EL performance in color-tunable OLEDs with a single Pt-emitter.[27,30] As depicted in **Figure 1**a,b, a color-tunable EL profile can be observed in a traditional co-host device structure of ITO/ HAT-CN (10 nm)/TAPC (40 nm)/TCTA (10 nm) /TCTA: B3PYMPM: **Pt-X-3** (20 nm)/ B3PYMPM (10 nm)/TmPyPb (40 nm) /LiF (1.2 nm)/Al (100 nm) at both low (6 wt%) and high (12 wt%) dopant concentrations. In these devices, HAT-CN (1,4,5,8,9,11-hexaazatriphenylene

hexacarbonitrile) was used as the hole-injecting layer, TAPC (1,1-bis-(4-bis(4-methylphenyl)-amino-phenyl)-cyclohexane) as the hole-transporting layer, TCTA (4,4′,4″-tris(*N*-carbazolyl)-triphenylamine) as the electron/exciton-blocking layer, B3PYMPM (bis-4,6-(3,5-di-3-pyridylphenyl)-2-methylpyrimidine) as the hole/exciton-blocking layer (EBL) and TmPyPB (1,3,5-tri(*m*-pyrid-3-yl-phenyl)) as the electron-transporting layer. The mixture of TCTA and B3PYMPM at a weight ratio of 1:1 was used as the co-host in the EML.[34] At the low concentration of 6 wt%, the **Pt-X-3** monomer emission located at around 527 nm dominated the EL spectrum, while its aggregation emission (^{3}MMLCT emission), located at a lower-energy wavelength, decreased with an increase in driving voltage, leading to a color shift from CIE coordinates of (0.39, 0.57) at 3 V to (0.35, 0.60) at 11 V. A similar color shift from CIE coordinates of (0.54, 0.45) at 3 V to (0.35, 0.60) at 11 V was found for the **Pt-X-3** device with a higher Pt(II) dopant concentration of 12 wt% (**Figure 1**b). Despite the different dominant emission bands and the wider color-span range, the spectral shift trend for the device with 12 wt% **Pt-X-3** was the same as that of the one with 6 wt%.

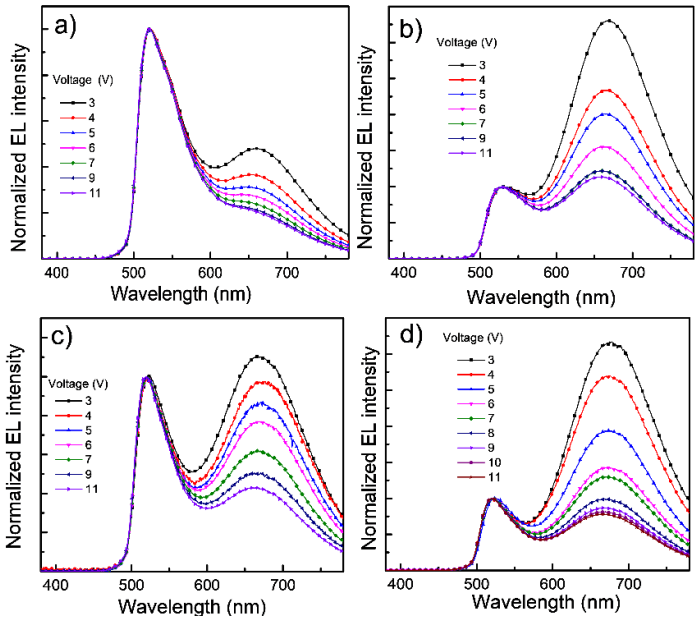

Figure 1. Normalized EL spectra at the indicated driving voltages, ranging from 3 to 11 V, for color-tunable OLEDs with EMLs consisting of a) TCTA: B3PYMPM: **Pt-X-3** (20 nm, 6 wt%), b) TCTA: B3PYMPM: **Pt-X-3** (20 nm, 12 wt%), c) TCTA: B3PYMPM: **Pt-X-3** (10 nm, 6

wt%)/ TCTA: B3PYMPM: **Pt-X-3** (10 nm, 12 wt%) or d) TCTA: B3PYMPM: **Pt-X-3** (10 nm, 12 wt%)/ TCTA: B3PYMPM: **Pt-X-3** (10 nm, 6 wt%).

To quantitatively address the shift in EL spectrum of both **Pt-X-3** based devices, we applied "Gaussian" fitting to estimate the ratio of aggregation emission to monomeric emission. At a low driving voltage of 3 V, the EL spectrum of the device with 12 wt% **Pt-X-3** was dominated by the aggregation emission, with an integral area ratio ($A_{agg/mon}$) of 11.4:1. With the increase in applied voltage to 11 V, the $A_{agg/mon}$ declined to 3.66:1. On the other hand, the $A_{agg/mon}$ in the EL spectrum of the device with 6 wt% **Pt-X-3** was 1.64:1 at 3 V and dropped to 0.85:1 at 11 V. As depicted in **Figure S1** (Supporting Information), the current density of the **Pt-X-3** devices decreased with dopant concentration from 3 to 12 wt%, suggesting that charge-trapping is a primary emission mechanism for the **Pt-X-3**-based devices.[35] For charge-trapping OLEDs, excitons directly form and recombine on the emitting dopants without using the step of energy transfer from the electrically excited molecules of the host to the emitter. Compared to the devices based on energy transfer, the current density versus voltage characteristics of charge-trapping devices strongly depend on the dopant concentration because charge-trapping on emitting dopants decreases the charge carrier mobility in the EML. In addition, the photoluminescent (PL) spectrum of the sample with 12 wt% **Pt-X-3** in the TCTA: B3PYMPM co-host shown in **Figure S2**, Supporting Information, is quite different from the EL spectrum of **Pt-X-3** at the same doping concentration (Figure 1b); the monomer emission is much stronger than that of the aggregation emission in the PL spectrum while the aggregation emission is much stronger in the EL one. Such different spectral profile between PL and EL of **Pt-X-3** at the same dopant concentration suggests that charges are trapped in the aggregation states of **Pt-X-3** during the EL process. Therefore, we applied the trapping-and-energy-transfer model to simulate the emission mechanism of color-tunable OLEDs fabricated with a **Pt-X-3** single emitter. In a charge-trapping-controlled device, charged carriers are trapped and recombined at low-energy dopant (aggregated **Pt-X-3**, here) when low voltage is applied,

leading to an EL spectrum dominated by aggregation emission. With the increase in driving voltage, the low-energy traps are gradually filled by increased injected carriers until saturation. At this stage, the high-energy emission from the excitons recombined at the high-energy dopant (monomeric **Pt-X-3**, in this case) gradually increases. Thus, the emission ratio $A_{agg/mon}$ decreases with the increasing driving voltage. Such a trapping-and-energy-transfer model can be expressed by **Equation 1**.

$$q(U) = \frac{D}{\mu}\left(\frac{d}{L_T}\right)^2 \frac{1}{U-U_0} + \frac{d}{L_T} \qquad (1)$$

Equation 1 was derived for single-layer polymer OLEDs by Meerholz and co-workers,[21] and applied by Wang and co-workers to multilayer OLEDs to account for color-tunable OLEDs.[22] Instead of merely using the intensity ratio of different emission bands, as in previous literature reports,[21,22] here we used the integral area ratio $A_{agg/mon}$ to describe the emission ratio q(U) in Equation 1. We employed this methodology because the full width at half maximum (FWHM) of the aggregated emission of **Pt-X-3** is greater than that of the monomer emission, which can cause a severe deviation during the simulation if the intensity ratio is used to describe q(U). In Equation 1, D is the diffusion coefficient of the trapped electrons, μ the mobility of the carriers, d the thickness of the EML, L_T the average diffusion distance before a carrier reaches a trapping center, U the driving voltage, and U_0 the built-in electronic field. D/μ is the Einstein relation that describes the ratio between diffusivity and mobility. By using Equation 1 to fit the experimental data from the device with 12 wt% **Pt-X-3**, the curve fitting matches the experimental data with a correlation coefficient R^2 of 0.96, as shown in **Figure 2**. This result validates the trapping-and-energy-transfer model in describing the EL process in **Pt-X-3** devices. Here, we obtained a built-in field U_0 of 2.2 V and an Einstein relation D/μ of 1.2, which is close to that reported in conventional organic systems.[21,22] For the device with 6 wt% **Pt-X-3**, the correlation coefficient R^2, built-in field U_0, and Einstein relation D/μ were 0.91, 2.2 V, and 1.2, respectively. It is notable that such a color-shift EL of **Pt-X-3** in the TCTA: B3PYMPM

host was not applicable for a random host. As depicted in **Figure S3** (Supporting Information) the EL spectrum was stable at low dopant concentration while slightly shifted at high dopant concentration, with increased driving voltage, when the mixture of TCTA:2,4,6-tris(biphenyl-3-yl)-1,3,5-triazine (T2T) was used as the co-host to replace TCTA: B3PYMPM, probably due to the relatively higher-lying HOMO (highest occupied molecular orbital) level of T2T,[36] in which the aggregation form of **Pt-X-3** was unable to trap charges effectively. Similarly, stable white emission has been reported for **Pt-X-2** OLEDs with the TCTA: 2,6-bis(3-(9H-carbazol-9-yl)phenyl)pyridine (26DCzPPy) co-host,[37] while color-tunable white emission could be realized when TCTA: 26DCzPPy was replaced by TCTA: B3PYMPM as the co-host in the EML.[27] The details of this color-tunable white device is discussed below.

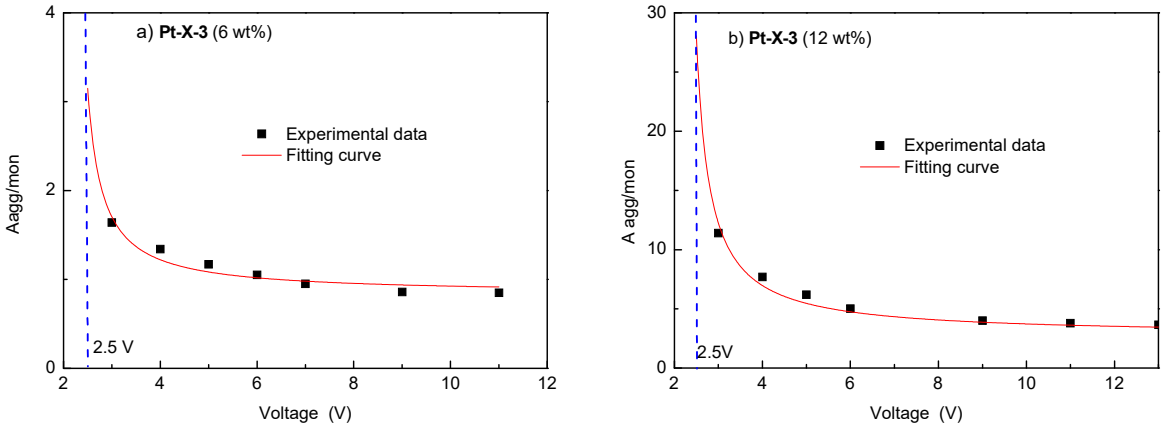

Figure 2. The dependence of $A_{agg/mon}$ on driving voltage of traditional co-host OLEDs with a **Pt-X-3** emitter at the indicated doping concentrations of 6 and 12 wt%. Solid squares represent experimental data, the solid red lines represent theoretical fitting results, and the blue dashed lines indicate the turn-on voltage of both devices.

Since the ratio of aggregated/monomer states of **Pt-X-3** was fixed at a fixed dopant concentration, the color-span would be limited within a relatively narrow spectral range, if a traditional co-host device structure was used. To further widen the color-span range of the **Pt-X-3** devices, we designed a novel co-host in double-emissive layer (CHIDEL) device structure by combining two mechanisms that enable color-tunable devices: recombination-zone-shift and trapping-and-energy-transfer. In CHIDEL devices, the single EML in traditional co-host

devices is replaced by two consecutive sub-EMLs with the same co-host system, but different dopant concentrations. In our case, the CHIDEL device structure was ITO/ HAT-CN (10 nm)/TAPC (40 nm)/TCTA (10 nm) /TCTA: B3PYMPM: **Pt-X-3** (x wt%, 10 nm)/ TCTA: B3PYMPM: **Pt-X-3** (y wt%, 10 nm)/ B3PYMPM (10 nm)/TmPyPb (40 nm) /LiF (1.2 nm)/Al (100 nm). A bilayer TCTA: B3PYMPM: **Pt-X-3** (x wt%, 10 nm)/ TCTA: B3PYMPM: **Pt-X-3** (y wt%, 10 nm) was used as the EML while x and y represent the doping concentrations of **Pt-X-3** in the two sub-EMLs. Two concentration (x/y) combinations of 6/12 and 12/6 were examined; the normalized EL spectra at different driving voltages are shown in Figure 1c, d. At a low driving voltage of 3 V, the EL spectrum of the 12/6 CHIMEL device was almost identical to that of the 12 wt% co-host device, suggesting that the excitons mainly formed in the sub-EML, adjacent to the TCTA layer, in the 12/6 CHIMEL device. With increasing driving voltage, the intensity of the **Pt-X-3** monomer emission quickly increased, and its relative intensity was much stronger than that of the 12 wt% co-host device at a high voltage of 11 V (Figure 1b, d), which is attributable to the expansion of the recombination zone to the 6 wt% sub-EML. For the 6/12 CHIMEL device, on the other hand, the relative intensity of the aggregation emission at the low driving voltage of 3 V was stronger than that of 6 wt% co-host device (Figure 1a, c). Such a stronger aggregation emission may be the result of the stronger trapping effect of the 12 wt% sub-EML, leading to an inferior color-span range when compared to that of the 12/6 CHIMEL device.

Despite the wide color-span range of the **Pt-X-3** device with the optimized CHIDEL structure, the following weaknesses of **Pt-X-3** limited its application: 1) The monomer emission (527 nm) of **Pt-X-3** is not blue enough to produce a "true" white light spectral profile when combined with its lower-energy aggregation emission, limiting its application in illumination devices, and 2) The photoluminescence quantum yields (PLQYs; 73.9% and 80.8% at 12 and 6 wt%, respectively; **Table 1**) of **Pt-X-3** in the film of TCTA:B3PYMPM double hosts are not high enough. For this reason, we applied two additional tetradentate Pt(II) complexes **Pt-X-2**

and **Pt-X-4** as single emitter in color-tunable OLEDs with CHIDEL structure, because of the higher energy of monomer emission of the former[25,27,30] and the higher PLQY of the latter.[30] The optimized EML structure for **Pt-X-2** was TCTA: B3PYMPM: **Pt-X-2** (26 wt%, 10 nm)/ TCTA: B3PYMPM: **Pt-X-2** (8 wt%, 10 nm), while that for **Pt-X-4** was TCTA: B3PYMPM: **Pt-X-4** (18 wt%, 10 nm)/ TCTA: B3PYMPM: **Pt-X-4** (8 wt%, 10 nm). Normalized EL spectra of **Pt-X-2** and **Pt-X-4** devices at various driving voltages are shown in **Figures 3**a and **3**b, respectively. The emission color of the **Pt-X-2** device shifted from yellowish-white to greenish-white, with CIE coordinates from (0.47, 0.44) to (0.36, 0.48), when the driving voltage increased from 3 to 11 V (Figure 3c). Of note, a high color rendering index (CRI) of 82 was achieved at 5 V. Similar to that of the **Pt-X-3** device, the emission color of the **Pt-X-4** device shifted from orange, with CIE coordinates of (0.56, 0.43), to yellowish-green, with CIE coordinates of (0.42, 0.55), with increasing driving voltage from 3 to 11 V. As shown in Figure 3c, the color-span range of **Pt-X-2** device is relatively narrow when compared to the **Pt-X-3** and **Pt-X-4** devices. PL spectra of 100-nm-thick films with **Pt-X-2** (26 wt%) **and Pt-X-4** (18 wt%) in TCTA: B3PYMPM co-host are shown in **Figure S5**, Supporting Information. Profound difference between the PL and EL spectra could be observed for **Pt-X-4** while only slight difference between PL and EL spectra of **Pt-X-2**, suggesting that trapping-and-energy-transfer mechanism plays an important role in the color-tuning process of the **Pt-X-4** device with a CHIDEL stucutre while the shift of recombination zone may be the main mechanism for the **Pt-X-2** device with a CHIDEL stucutre.

The EQE-luminance characteristics of the devices with **Pt-X-2**, **Pt-X-3**, and **Pt-X-4** are depicted in **Figure 4**a; maximum EQEs of 20.75, 20.67, and 23.23% were achieved, respectively. At a high luminance of 1000 cd m^{-2}, the EQE of the **Pt-X-3** device slightly decreased to 20.58%, corresponding to an efficiency roll-off of less than 2%. For the **Pt-X-4** device, a maximum EQE of 23.23% was achieved at 1300 cd m^{-2}. At higher luminance of 5000 and 10000 cd m^{-2}, the efficiency roll-offs of both the **Pt-X-3** and **Pt-X-4** devices were small, at

8.73% and 15.50% for the former and 9.38% and 19.97% for the latter, respectively. Compared to the **Pt-X-3** and **Pt-X-4** devices, the efficiency roll-off of the **Pt-X-2** device was profound at high luminance beyond 2000 cd m^{-2}, being 49.5% and 67.8% at 5000 and 10000 cd m^{-2}, respectively. We attribute such strong efficiency roll-off of the **Pt-X-2** device to the long emission lifetime of **Pt-X-2** monomer. The emission lifetimes of monomer and aggregate states of **Pt-X-2** are 11.5 and 2.4 μs, respectively.[30] With increased luminance, the monomer emission of the **Pt-X-2** device became stronger (see Figure 3a) and the device efficiency strongly dropped that was caused by triplet-triplet annihilation due to the longer emission lifetime of **Pt-X-2** monomer. In addition to comparing the EQE at high luminance, typically 1000 cd m^{-2}, with the maximum EQE, the critical current density J_{90}, *i.e.* the current density at which the EQE drops to 90% of its maximum value,[38] can also be used to evaluate the efficiency roll-off of OLEDs. In our case, as depicted in **Figure S4**, J_{90} was 0.28, 23.51, and 14.92 mA cm^{-2} for the devices with **Pt-X-2**, **Pt-X-3**, and **Pt-X-4**, respectively.

In addition to PLQY, the EQE value of an OLED is also a function of the out-coupling efficiency, which is strongly influenced by the horizontal transition dipole moment of the EML.[39] A horizontal transition dipole moment has been observed in several OLEDs based on Ir(III) and Pt(II) complexes.[40] Angular distributions of the EL intensities of **Pt-X-4** in conventional TCTA: B3PYMPM co-host OLEDs with different dopant concentrations of 8 and 18 wt% were measured, and the results are shown in Figure 4b. The EL distributions for both dopant concentrations did not match the Lambert distribution; a weak micro-cavity effect could be observed in the device with the lower concentration of **Pt-X-4**, while a pattern related to horizontal molecular orientation appeared when the concentration increased to 18 wt%.[29,41-43] Such different EL angle distributions at different concentrations of **Pt-X-4** suggest that the horizontal molecular direction is preferred in the aggregation states of **Pt-X-4**. As shown in **Figure S6**a, Supporting Information, the phenomenon that the emission intensity of aggregation states of **Pt-X-4** increased with increasing angle relative to that of the monomer emission could

be a result of the different horizontal dipole ratio (Θ) between monomer and aggregation states of **Pt-X-4**. By assuming the charge balance factor as 1, the out-coupling efficiency of a phosphorescent OLED can be calculated by its EQE and PLQY of its EML.[39] As depicted in Figure S6b, Supporting Information, the EQEs of the **Pt-X-4** devices with dopant concentrations of 8 and 18 wt% were 22.09% and 26.05%, respectviely. Accrording to the PLQY values of 96.1% (8 wt%) and 91.8% (18 wt%) for corresponding EMLs (see Table 1), the out-coupling efficiencies were estimated to be 22.98 and 28.38% for the devices with 8 and 18 wt% **Pt-X-4**, respectively. The high out-coupling efficiencies suggest horizontally aligned Θ (Θ > 0.67) for both EMLs. Since the co-host TCTA:B3PYMPM used in these devices has been proved to be horizontally aligned,[39] the contribution of emitting dopants to Θ can hardly be quantitatively calculated. Nonetheless, the relative higher out-coupling efficiency for the device with 18 wt% **Pt-X-4** indicates that the aggregation states of **Pt-X-4** could be more favorable to enhance Θ of the EML.

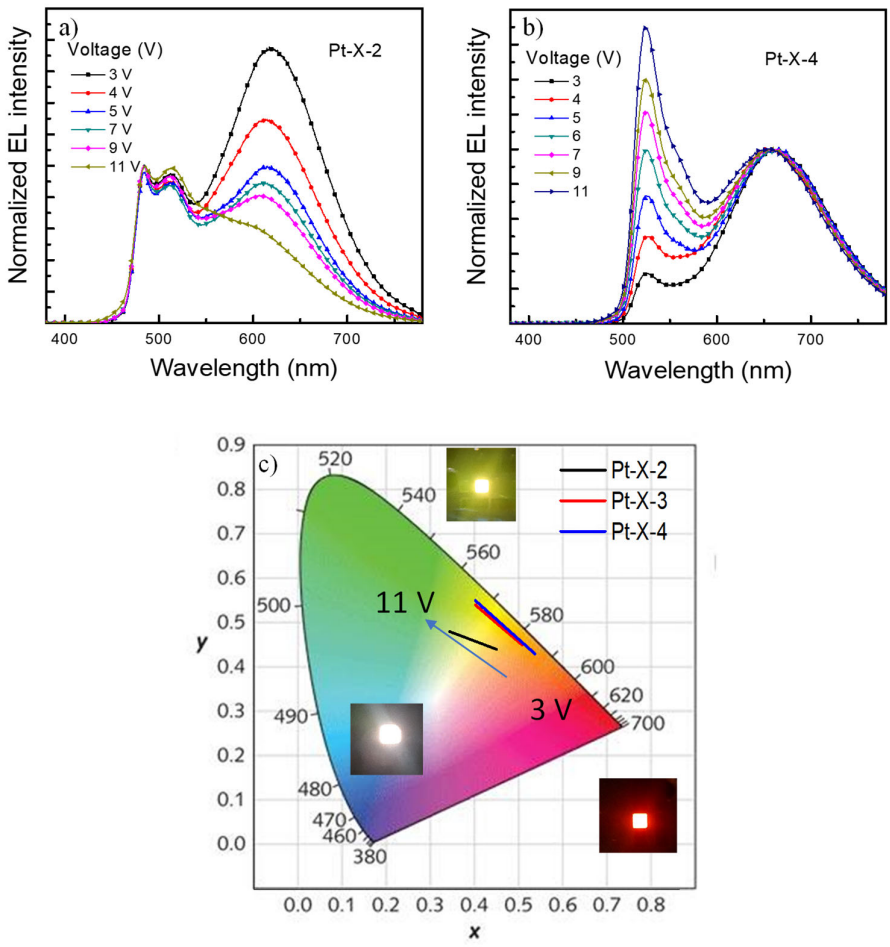

Figure 3. Normalized EL spectra of color-tunable OLEDs with CHIDEL structure based on a) **Pt-X-2** and b) **Pt-X-4**. c) Color-shift of OLEDs with **Pt-X-2**, **Pt-X-3** and **Pt-X-4**, upon increasing driving voltage.

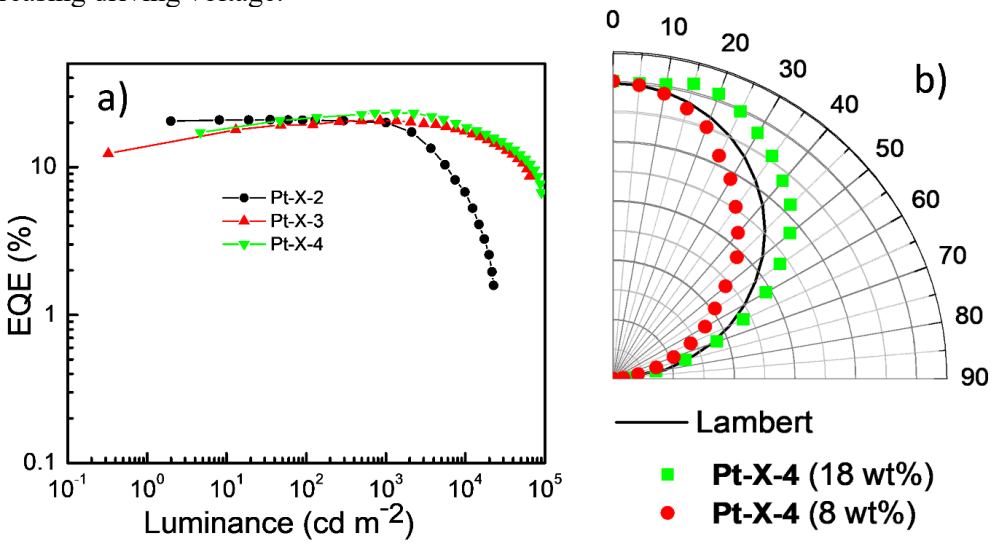

Figure 4. a) EQE-luminance characteristics of color-tunable OLEDs with **Pt-X-2**, **Pt-X-3** and **Pt-X-4**. b) EL patterns of **Pt-X-4** in OLEDs with conventional single EMLs with co-host TCTA: B3PYMPM at 8 and 18 wt%; the solid black line represents the Lambert distribution.

Table 1. Key performance characteristics of color-tunable OLEDs with CHIDEL structure

Emitter (x/y)[a]	L[b] (cd m^{-2})	EQE (%)		CE (cd A^{-1})		PE (lm W^{-1})		PLQY[c] (%)	CIE (x, y)	
		Max	at 1000 cd m^{-2}	Max	at 1000 cd m^{-2}	Max	at 1000 cd m^{-2}		at 3 V	at 11 V
Pt-X-2 26 wt%/8 wt%	22680	20.81	19.96	43.88	42.18	50.18	24.28	75.5/68.1	0.47, 0.44	0.36, 0.48
Pt-X-3 12 wt%/6 wt%	64766	20.61	20.58	26.95	25.88	17.72	14.51	73.9/80.8	0.53, 0.45	0.42, 0.54
Pt-X-4 18 wt%/8 wt%	90530	23.23[d]	23.19	43.71	40.08	29.15	26.58	91.8/96.1	0.56, 0.43	0.42, 0.55

[a] Concentration of the Pt-emitter in the two sub-EMLs; [b] Luminance at 11 V; [c] PLQY values in the two sub-EMLs; [d] Maximum EQE was achieved at a luminance greater than 1000 cd m^{-2}.

We conducted a preliminary examination of the operational stability of the OLEDs with **Pt-X-4** under laboratory conditions. The duration to drop to 90% of the initial luminance (LT_{90}) of the **Pt-X-4** OLEDs was 13.95 h (see **Figure S7**, Supporting Information). Considering the initial luminance (L_0) of 7000 cd m^{-2}, LT_{90} at the L_0 of 100 cd m^{-2} for the **Pt-X-4** device was estimated to be 19105 h. (As sensors, these color-tunable devices could function at around 100 cd m^{-2}.)

In conclusion, we have designed a novel CHIDEL device structure for color-tunable OLEDs based on a single tetradentate Pt(II) emitter by combining recombination-zone-shift and trapping-and-energy-transfer mechanisms. Wide color-span range, high efficiency and low-efficiency roll-off were achieved in the CHIDEL devices based on **Pt-X-2**, **Pt-X-3** and **Pt-X-4**. The EL distribution and long-term operational stability of **Pt-X-4**-based devices were also examined. The results show that the aggregation states of **Pt-X-4** were horizontally oriented in the EML, and the device lifetime LT_{90} was almost 20000 h at the functional luminance of sensors. Owing to the high efficiency and decent stability, simple-structured, color-tunable OLEDs with **Pt-X-4** may find applications in wearable biomedical devices, such as real-time electrocardiogram monitors.

Experimental Section

Materials: HAT-CN, TAPC, TCTA, B3PYMPM, T2T and TmPyPb were purchased from Luminescence Technology Corp. All of these materials were used as received. **Pt-X-2**, **Pt-X-3** and **Pt-X-4** were synthesized as described previously[25,27,43] and purified by gradient sublimation before use.

PLQY measurement: Samples of Pt(II) complexes doped in TCTA: B3PYMPM co-host at a suitable ratio were prepared by co-deposition in a Kurt J. Lesker SPECTROS vacuum deposition system with a base pressure of 10^{-8} mBar. The substrate was a 1 cm × 1 cm quartz plate, and the thickness was 100 nm for all samples. The emission spectra and emission quantum efficiency of the thin films were assessed using a Hamamatsu absolute PL quantum yield spectrometer C11347.

Device Fabrication and Characterization: OLEDs were fabricated in a Kurt J. Lesker SPECTROS vacuum deposition system with a base pressure of 10^{-8} mBar. In the vacuum chamber, organic materials were thermally deposited in sequence at a rate of ≈0.1 nm s^{-1}. The doping process in the emitting layer was realized by co-deposition technology. Afterward, LiF (1.2 nm) and Al (100 nm) were thermally deposited at rates of 0.03 and 0.2 nm s^{-1}, respectively. Film thicknesses were determined *in situ* using calibrated oscillating quartz crystal sensors.

EL spectra, *J-L-V* characteristics, CIE coordinates, CRI, EQE, CE and PE were measured using a Keithley 2400 source-meter and an absolute external quantum efficiency measurement system (C9920-12, Hamamatsu Photonics). EL distribution was measured with an angle-dependent device testing system (C9920-11, Hamamatsu Photonics). All devices were characterized at room temperature without encapsulation.

Device lifetime measurement: The OLEDs used to evaluate the long-term stability of **Pt-X-4** had a device structure of ITO/HAT-CN (5 nm)/ NPB (20 nm)/ FSFA (15 nm)/ DMIC-TRZ: DMIC-CZ: **Pt-X-4** (8 wt%) / ANT-BIZ (20 nm)/ Liq (1 nm)/ Al (100 nm). The chemical structures of NPB, FSFA, DMIC-TRZ, DMIC-CZ, ANT-BIZ, and Liq are depicted in **Scheme S1**, Supporting Information. All materials except for **Pt-X-4** were purchased from PURI

materials (Shenzhen, China). They were used as received without further purification. The OLEDs were fabricated in a Kurt J. Lesker SPECTROS vacuum deposition system and encapsulated in a 200-nm-thick Al_2O_3 thin film deposited by atomic layer deposition (ALD) in a Kurt J. Lesker SPECTROS ALD system.

Supporting Information
Supporting Information is available from the Wiley Online Library or from the author.

Acknowledgments
This work was supported by the Guangdong Major Project of Basic and Applied Basic Research (2019B030302009), Science Technology and Innovation Commission of Shenzhen Municipality (JCYJ 20170818141858021, JCYJ 20170412140251576, JCYJ 20180508162429786), Innovation and Technology Fund (ITS/224/17FP), and Innovation and Technology Commission, Centre of Machine Learning for Energy Materials and Devices, a major initiative–Artificial Intelligence and Robotics cluster under InnoHK (AIR@InnoHK).
Received: ((will be filled in by the editorial staff))
Revised: ((will be filled in by the editorial staff))
Published online: ((will be filled in by the editorial staff))

Reference:

[1] J. Kido, M. Kimura, K. Nagai, *Science* **1995**, *267*, 1332.
[2] S. Reineke, F. Lindner, G. Schwartz, N. Seidler, K. Walzer, B. Lüssem, K. Leo, *Nature* **2009**, *459*, 234.
[3] S. Reineke, M. Thomschke, B. Lüssem, K. Leo, *Rev. Mod. Phys.* **2013**, *85*, 1245.
[4] G. M. Farinola, R. Ragni, *Chem. Soc. Rev.* **2011**, *40*, 3467.
[5] M. C. Gather, A. Köhnen, K. Meerholz, *Adv. Mater.* **2011**, *23*, 233.
[6] Z. Chen, C. L. Ho, L. Wang, W. Y. Wong, *Adv. Mater.* **2020**, *32*, 1903269.
[7] C. W. Tang, S. A. VanSlyke, *Appl. Phys. Lett.* **1987**, *51*, 913.
[8] Y. Ma, H. Zhang, J. Shen, C. Che, *Synth. Met.* **1998**, *94*, 245.
[9] Z. Shen, P. E. Burrows, V. Bulović, S. R. Forrest, M. E. Thompson, *Science* **1997**, *276*, 2009.
[10] M.-H. Huang, W.-C. Lin, C.-C. Fan, Y.-S. Wang, H.-W. Lin, J.-L. Liao, C.-H. Lin, Y. Chi, *Org. Electron.* **2015**, *20*, 36.
[11] J. N. Arthur, D. P. Forrestal, M. A. Woodruff, A. K. Pandey, S. D. Yambem, *ACS Photonics* **2018**, *5*, 2760.
[12] M. Li, X. Zhang, H. Zhang, W. Chen, L. Ma, X. Wang, Y. Liu, B. Lei, *J.Mater.Chem.C* **2019**, *7*, 3617.
[13] J. H. Koo, S. Jeong, H. J. Shim, D. Son, J. Kim, D. C. Kim, S. Choi, J.-I. Hong, D.-H. Kim, *ACS nano* **2017**, *11*, 10032.
[14] C. Wang, D. Hwang, Z. Yu, K. Takei, J. Park, T. Chen, B. Ma, A. Javey, *Nat.Mater.* **2013**, *12*, 899.
[15] G. Parthasarathy, G. Gu, S. R. Forrest, *Adv. Mater.* **1999**, *11*, 907.
[16] Y. Jiang, J. Lian, S. Chen, H.-S. Kwok, *Org. Electron.* **2013**, *14*, 2001.
[17] M. Fröbel, T. Schwab, M. Kliem, S. Hofmann, K. Leo, M. C. Gather, *Light: Science & Applications* **2015**, *4*, 247.

[18] K. M.-C. Wong, X. Zhu, L.-L. Hung, N. Zhu, V. W.-W. Yam, H.-S. Kwok, *Chem. Commun.* **2005**, 2906.
[19] S. Liu, R. Wu, J. Huang, J. Yu, *Appl. Phys. Lett.* **2013**, *103*, 181.
[20] J.-H. Jou, M.-H. Wu, S.-M. Shen, H.-C. Wang, S.-Z. Chen, S.-H. Chen, C.-R. Lin, Y.-L. Hsieh, *Appl. Phys. Lett.* **2009**, *95*, 013307.
[21] M. C. Gather, R. Alle, H. Becker, K. Meerholz, *Adv.Mater.* **2007**, *19*, 4460.
[22] Q. Wang, J. Ding, D. Ma, Y. Cheng, L. Wang, X. Jing, F. Wang, *Adv. Func. Mater.* **2009**, *19*, 84.
[23] G. Cheng, K. T. Chan, W. P. To, C.-M. Che, *Adv. Mater.* **2014**, *26*, 2540.
[24] D. Luo, Q. Chen, Y. Gao, M. Zhang, B. Liu, *ACS Energy Lett.* **2018**, *3*, 1531.
[25] G. Cheng, P. K. Chow, S. C. Kui, C. C. Kwok, C.-M. Che, *Adv. Mater.* **2013**, *25*, 6765.
[26] T. Fleetham, J. Ecton, Z. Wang, N. Bakken, J. Li, *Adv. Mater.* **2013**, *25*, 2573.
[27] G. Cheng, S. C. Kui, W.-H. Ang, M.-Y. Ko, P.-K. Chow, C.-L. Kwong, C.-C. Kwok, C. Ma, X. Guan, K.-H. Low, *Chem. Sci.* **2014**, *5*, 4819.
[28] G. Li, T. Fleetham, J. Li, *Adv. Mater.* **2014**, *26*, 2931.
[29] D. Zhang, J. Qiao, D. Zhang, L. Duan, Adv. Mater. **2017**, 29,1702847.
[30] G. Cheng, Q. Wan, W. H. Ang, C. L. Kwong, W. P. To, P. K. Chow, C. C. Kwok, C.-M. Che, *Adv. Opt. Mater.* **2018**, 1801452.
[31] K. H. Kim, J. L. Liao, S. W. Lee, B. Sim, C. K. Moon, G. H. Lee, H. J. Kim, Y. Chi, J. J. Kim, *Adv. Mater.* **2016**, *28*, 2526.
[32] K. T. Ly, R.-W. Chen-Cheng, H.-W. Lin, Y.-J. Shiau, S.-H. Liu, P.-T. Chou, C.-S. Tsao, Y.-C. Huang, Y. Chi, *Nat. Photonics* **2017**, *11*, 63.
[33] P. K. Chow, G. Cheng, G. S. M. Tong, W. P. To, W. L. Kwong, K. H. Low, C. C. Kwok, C. Ma, C.-M. Che, *Angew. Chem. Int. Ed.* **2015**, *54*, 2084.
[34] Y. S. Park, S. Lee, K. H. Kim, S. Y. Kim, J. H. Lee, J. J. Kim, *Adv. Funct. Mater.* **2013**, *23*, 4914.
[35] R. Holmes, B. D'Andrade, S. Forrest, X. Ren, J. Li, M. Thompson, *Appl. Phys. Lett.* **2003**, *83*, 3818.
[36] H.-F. Chen, S.-J. Yang, Z.-H. Tsai, W.-Y. Hung, T.-C. Wang, K.-T. Wong, *J. Mater. Chem. C* **2009**, *19*, 8112.
[37] Y. J. Doh, J. S. Park, W. S. Jeon, R. Pode, J. H. Kwon, *Org. Electron.*, 2012, **13**, 586.
[38] M. A. Baldo, C. Adachi, S. R. Forrest, *Phys. Rev. B* **2000**, *62*, 10967.
[39] S. Y. Kim, W. I. Jeong, C. Mayr, Y. S. Park, K. H. Kim, J. H. Lee, C. K. Moon, W. Brütting, J. J. Kim, *Adv. Funct. Mater.* **2013**, *23*, 3896.
[40] T. D. Schmidt, T. Lampe, P. I. Djurovich, M. E. Thompson, W. Brütting, *Phy. Rev. Appl.* **2017**, *8*, 037001.
[41] J. Kim, T. Batagoda, J. Lee, D. Sylvinson, K. Ding, P. J. Saris, U. Kaipa, I. W. Oswald, M. A. Omary, M. E. Thompson, *Adv. Mater.* **2019**, *31*, 1900921.
[42] N. Jiang, H.-N. Yang, J.-X. Man, T. Zhang, S.-J. He, D.-K. Wang, Z.-H. Lu, *Org. Electron.* **2020**, ***78***, 105611.
[43] J. Lin, Y. Hu, X. Liu, *Adv. Opt. Mater.* **2020**, *8*, 1901421.
[44] S. C. Kui, P. K. Chow, G. Cheng, C.-C. Kwok, C. L. Kwong, K.-H. Low, C.-M. Che, *Chem. Commun.* **2013**, *49*, 1497.

The table of contents entry

Mao Mao, Tsz Lung Lam, Wai-Pong To, Xiang-Zhou Lao, Weiqiang Liu, Shi-Jie Xu, Gang Cheng*, Chi-Ming Che*

Stable, High-Efficiency Voltage-Dependent Color-Tunable Organic Light-Emitting Diodes with a Single Tetradentate Platinum(II) Emitter Having Long Operational Lifetime

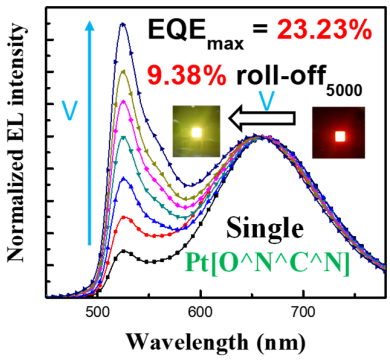

High-performance voltage-dependent color-tunable OLEDs with a single Pt[O^N^C^N] emitter are fabricated. The emission color can be tuned from warm white to nature white or from orange to yellowish green upon the emitter used. High EQE (23.23%), low efficiency roll-off, long-term stability (LT_{90}=19105 h) and continuously variable color enable these color-tunable OLEDs to find applications in smart wearable devices.